Chinese Journal of Polar Science, Vol 20, No 2, 187－199, December 2009

Shock metamorphism of ordinary chondrites from Grove Mountains, Antarctica

Feng Lu(冯璐)[1], Lin Yangting(林杨挺)[1], Hu Sen(胡森)[1] and Liu Tao(刘焘)[2]

1 Institute of Geology and Geophysics, Chinese Academy of Science, Beijing 100029, China

2 Guangzhou Institute of Geochemistry, Chinese Academy of Science, Guangzhou 510640, China

Received December 20, 2009

Abstract Shock effects of 93 Grove Mountains (GRV) ordinary chondrites were studied in this work, including fracture, various types of extinction, and recrystallization of silicates observed under optical microscopy. Shock-induced veins and pockets show various microtextures, decomposition and phase transformation of minerals. The confirmed high-pressure polymorphs of silicates are ringwoodite, majorite, pyroxene glass and maskelynite. Based on the shock effects and assemblages of high-pressure minerals, shock stages of all of 93 GRV chondrites were classified. In comparison with literature, the Grove Mountains meteorites have a higher fraction (23 out of 93) of heavily shocked samples (S4—S5). Most of the heavily shocked meteorites are L group (22 out of 23), except for one H chondrite. The distinct shock metamorphism between H and L groups may indicate different surface properties of their parent bodies. In addition, there is relationship between petrologic types and shock stages, with most heavily shocked samples observed in equilibrated ordinary chondrites (especially Type 5 and 6).

Keywords Antarctic, Grove Mountains, chondrites, shock metamorphism, high-pressure mineral

1 Introduction

Shock metamorphism and brecciation resulting from hypervelocity collisions on their parent bodies are the most common features of meteorites[1]. Shock effects including deformation, melting and decomposition of mineral components are recorded. Moreover, natural high-pressure polymorphs of rock-forming minerals were also discovered in heavily shocked meteorites. Since the high pressures and temperature conditions during shock events are comparable to those of Earth's transition zone, or the lower mantle, the study of shock effects in meteorites is of great importance, not only to decipher the collisional and geological history of their asteroidal parent bodies, but also to acquire the information of the dynamics and properties of the deep Earth.

Based on the shock effects in silicate minerals and shock-induced localized melting in ordinary chondrites, seven stages of shock metamorphism (S1—S6 and shock melted) were classified by Stöffler *et al*[2], the P-T conditions of every shock stage were given as well

However, great improvements in high-pressure field have been achieved in recent ten years, that static high-pressure experiments were introduced to study the transformation conditions of high-pressure minerals in shocked meteorites, whereafter the P-T-t conditions of shock events were modified. These developments provide new knowledge of the shock history of parent body of meteorites, as well as the study of the constitutes of the deep Earth[3-5].

In this study, we observed and described shock effects in 93 Grove Mountains ordinary chondrites, which were recovered from Grove Mountains, Antarctic in 2005. Shock stages were classified, and the history of shock events were also discussed based on the high-pressure polymorphs discovered in these samples.

2 Sample and Experiment

Polished thin sections of the 93 ordinary chondrites were examined with an optical microscope in transmitted and reflected light. The shock-induced veins and pockets were carefully observed by an LEO 1450VP Scanning Electronic Microscope (SEM). The major element composition of the minerals in the melt veins and pockets were also checked for their major element composition by energy dispersive spectroscopy (EDX) on the SEM.

A RM-2000 Laser Raman spectrometer was hired to identify the high pressure polymorphs of minerals. The 514 nm excitation beam from the Ar+ laser was focused to 1 μm spot on the selected grains. The accumulations of the signal last 10 s, partly 15 s. The quantitative chemical analysis of the selected grains was conducted using a JEOL JXA-8100 electron microprobe at 15 kV accelerating voltage and 20 nA beam current.

3 shock-induced effects

3.1 Undulose extinction

The weakest observable shock effects in olivine are undulatory extinction, which can be easily distinguished under cross-polarized light from sharp, uniform extinction of unshocked olivine by the fact that the former, the extinction position of a single crystal varies systematically across the grain, with the rotation of the sample stage (Fig. 1a).

With increasing shock, the olivine crystal structure is messed up even further, forming small (only a few micrometers) domains that differ in their extinction positions by more than 3 to 5° of rotation of the sample stage. This kind of mosaicism extinction is also observed in several severely shocked samples (Fig. 1b).

3.2 Planar Fractures

At the lowest shock category, olivine crystals have irregular cracks. With increasing shock pressure, the grains tend to develop planar fractures, which are parallel cracks lined up in one direction (Fig. 2a). There are often more than one set of fracturing in a single mineral crystal, and the cracks are oriented along crystallographic planes (Fig. 2b). Planar fractures were considered to be the most important shock indicators at moderate shock pressures[2].

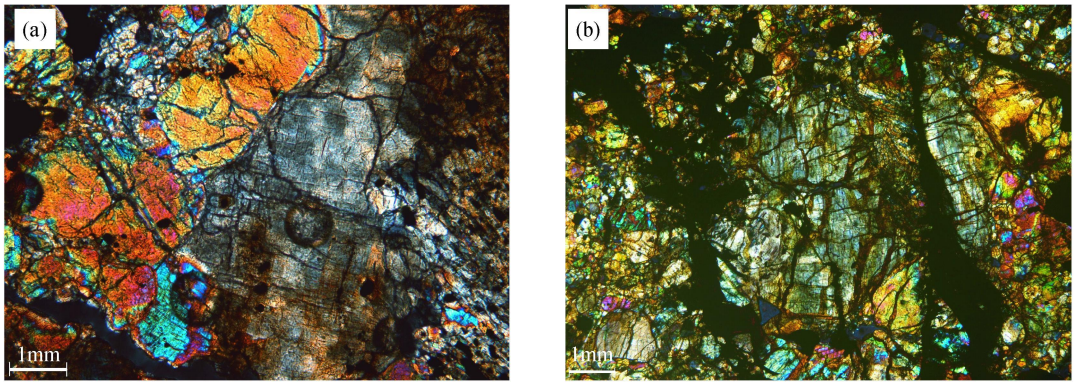

Fig. 1 (a) Photomicrograph of olivine in GRV052610 under cross-polarized light. The coarse grey to yellow and red grains are olivine. The grey-colored grain in the center of the view exhibits undulatory extinction and a set of planar fractures. The scale bar is 1 mm.
(b) Photomicrograph of olivine in GRV052610 under cross-polarized light. The grey grain of olivine in the center of the view shows mosaic extinction. The scale bar is 1 mm.

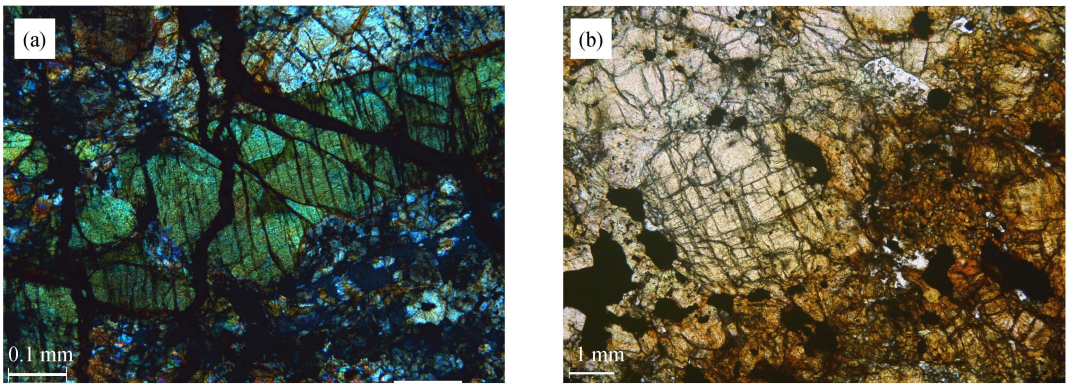

Fig. 2 (a) Photomicrograph of olivine in GRV052448 under cross-polarized light. The cyan large grain in the middle of the view is olivine, displaying a set of planar fractures. The scale bar is 0.1 mm.
(b) Photomicrograph of olivine in GRV051796 under plane-polarized light. The large grain on the left is olivine, exhibiting two sets of planar fractures nearly perpendicular to each other. The scale bar is 1 mm.

3.3 Shock-induced localized melting

3.3.1 Melting of metallic Fe-Ni and sulfide

GRV051773 (L group ordinary chondrite) contains a network of opaque veins while the silicates in host rock exhibit pervasive fractures and darkening. The shock-induced veins contain silicate hostrock fragments, from 10 to around 100 μm, in a matrix of metal-sulfide melt (Fig. 3). The angular to rounded shapes of the silicate fragments suggest that they are cataclastic fragments formed by extensive shear deformation.

The matrices of these veins consist of iron sulfide that was apparently liquid. These textures suggest that most of the veins in this sample were caused by frictional heating to temperatures high enough to melt the metal-sulfide component, but generally not high enough to melt the silicate. According to the study of shock metamorphism in enstatite chon-

drites by Rubin *et al*. the formation of these opaque metal-sulfide veins suggest a shock stage of above S3[6].

3.3.2 *Shock effects of silicates*

The process of shock-induced local melting generally involves simultaneous total melting of coexisting minerals, mixing and homogenization of the produced melts and the subsequent crystallization of immiscible silicate and sulfide/metal melts. Shock-induced veins appear as opaque veins or pockets macroscopically and in the polarizing microscope, with widths ranging from micrometer to millimeter-sized (Fig. 4). Several samples are covered by networks of interconnected shock veins. A few samples were severely shocked and molten, with networks of opaque veins covering the whole thin sections.

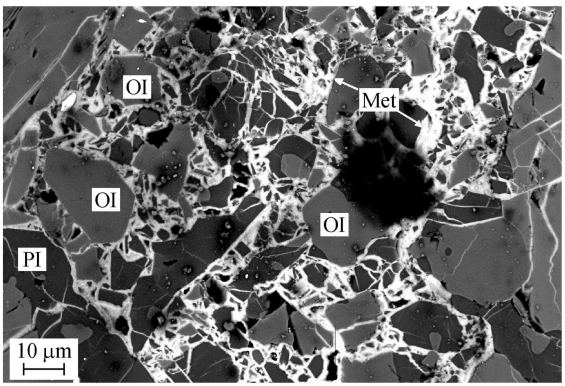

Fig. 3 BSE image of GRV051773, showing a shock-induced metal vein. The network veins are metal, and silicate fragments (note their sharp edges) are olivine and plagioclase (Pl). The scale bar is 10 μm.

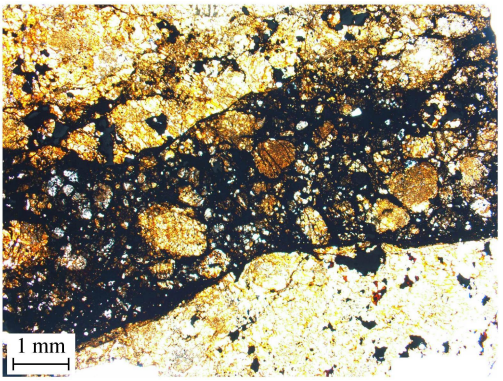

Fig. 4 Photomicrograph of shock-induced vein in GRV052174 under Plane-polarized light. Matrix of the shock-induced vein is opaque, and large silicate clasts are rounded in shapes with diameters of 20—60 μm. The scale bar is 1 mm.

Two distinct lithologies of the shock-induced veins can be seen by microscope under reflected light: coarse-grained mineral aggregates and fine-grained matrix. The fine-grained matrix is mainly consist of granular silicates and abundant spherules of eutectics of opaque minerals (Fe-Ni metal, sulfide, chromite etc). Cellular dendrites of Fe-Ni metal and troilite were observed in large spherules. The opaque minerals are usually dispersed into some regions of a blocky or belt shape (Fig. 5). On BSE image, the fine grained silicates in matrix are idiomorphic or needle-like crystals. The size of matrix grains is about 1-3 μm, and exhibit a decreasing trend from in the middle to the boundaries of the veins (Fig. 6). On BSE images, bright acicular crystals which are enriched in FeO were noticed inside the matrix. The chemical compositions of the idiomorphic grains, which are the main components of the matrix, were analyzed by the energy dispersive x-ray spectroscopy (EDS) on SEM. The results show that they have a composition of pyroxene ($(Mg, Fe)SiO_3$). Raman spectra of these grains indicated they are majorite-pyrope solid solution (Fig. 8a) that were crystallized from shock-induced chondritic melt under high pressures[3,7].

The large clasts and fragments enclosed in the shock-induced veins are rounded or ovoid (Fig. 4 and 5), most of which display full extinction cross-polarized light, indicative of the transformation of crystal structures under high pressure.

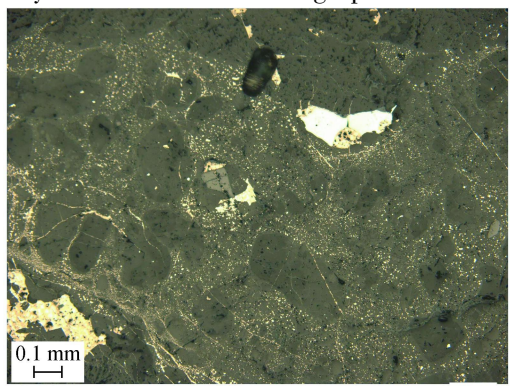

Fig. 5 Photomicrograph of a shock-induced vein in GRV 052049 under reflected light. The melt vein consists of fine-grained silicates (dark grey) and Fe-Ni metal and troilite (light grey or white spots), with numerous rounded silicate fragments. The scale bar is 0.1 mm.

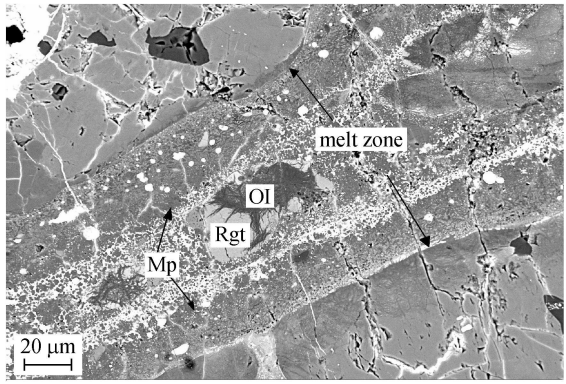

Fig. 6 Back-scattered electron (BSE) image of a shock-induced vein in GRV 052082. The matrix of the vein consists of garnet and needle-like majorite-pyrope (Mp), with small spherules or network of Fe-Ni metal and troilite intergrowth. Coarse-grained olivines in the middle of the vein have partially been transformed to ringwoodite (Rgt). Also note heterogeneous margins of olivine in contact with the vein. The scale bar is 20 mm.

3.4 High-pressure polymorphs of Olivine

Olivine is one of the main constituent minerals in ordinary chondrites. The natural high-pressure polymorphs of olivine, wadsleyite and ringwoodite, have been discovered in several shocked meteorites. The $(Mg, Fe)_2SiO_4$ phase diagram at high P-T conditions is well established from high-pressure experiments and show that olivine will transform into spinel-structured ringwoodite under 18—23 Gpa, 1800—1900℃[8,9].

In this study, olivine clasts are commonly observed in the shock-induced veins from most of the shocked samples. The shapes of entrained olivine fragments are ovoid, and consist of dark fiber-like cores (Fe-poor) and bright rims (Fe-rich) on BSE image (Fig. 7).

Raman analyses show that the dark cores are olivine, while the bright rims are ringwoodite (Fig 8b). EMPA results show a distinct difference in chemical compositions between ringwoodite and co-existing olivine. The ringwoodite rims are enriched in FeO, whereas the olivine cores are enriched in MgO (Table 1).

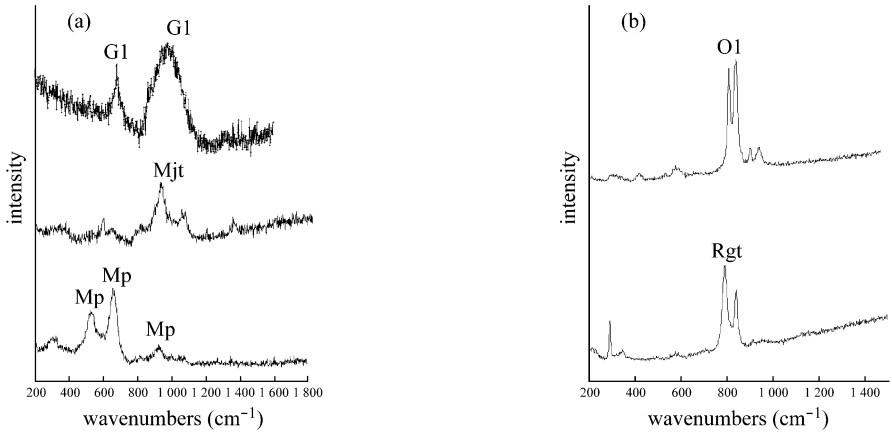

Fig 7 Back-scattered electron (BSE) image of a shock-induced vein in GRV052049, showing two round grains consisting of fiber-like olivine cores and ringwoodite (Rgt) rims. The ringwoodite is FeO-rich (ligh-grey), while olivine is FeO-poor (dark grey). The scale bar is 20 μm.

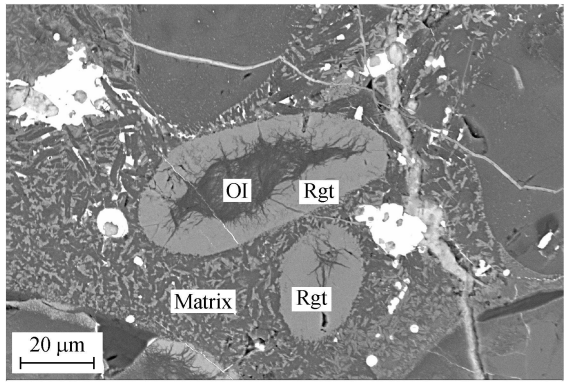

Fig 8 Raman spectra of minerals in shock-induced veins. (a) Mp majorite-pyrope; Mjt majorite; Gl pyroxene glass; (b) Rgt ringwoodite; Ol Olivine.

3.5 High-pressure polymorphs of Pyroxene

Ovoid pyroxene clasts were found in the shock-induced veins from GRV050418, GRV051674, GRV051876, GRV052082, GRV052174 and GRV052049. The clasts are composed of polycrystalline and amorphous areas, which display different brightness on BSE image (Fig. 9). The Microprobe analyses show there is no significant difference among chemical compositions of the dark and bright areas from one single grain.

The polycrystalline parts can be indentified as majorite (noncubic garnet, one of the high-pressure polymorphs of pyroxene) by the strong typical peak around 930 cm^{-1} observed by Raman spectroscopy (Fig. 8b). Raman spectra of the smooth amorphous parts

contain two broaden peaks around 670 and 970 cm^{-1} (Fig. 8a) that are in agreement with the identification of (Mg, Fe)SiO_3 glass in previous study[11-13]. (Mg, Fe)SiO_3 glass were observed to coexist with low-Ca pyroxene and majorite in a single clast. Clear boundaries can be seen on BSE images between (Mg, Fe)SiO_3 glassy phase and majorite, as the former are usually smooth and homogenous, whereas the latter often occur as sub-micron grains in decomposed rims of the clasts. EMPA results show that the chemical compositions of (Mg, Fe)SiO_3 glass are the same as low-Ca pyroxene in host rock.

Table 1. Selected Electron Microprobe Analyses of ringwoodite and olivine in melt zones (wt%). Rgt: ringwoodite, Ol: olivine

Grain	Mineral	SiO_2	TiO_2	Al_2O_3	Cr_2O_3	FeO	MnO	MgO	CaO	Na_2O	K_2O	P_2O_5	Total	Fa
1	Rgt	33.8	0.02	0.046	0.287	48.977	0.06	16.42	n.d.	n.d.	n.d.	n.d.	99.613	62.6
	Ol	41.85	0.029	0.006	0.05	7.948	0.175	50.57	0.031	n.d.	0.014	n.d.	100.67	8.1
2	Rgt	36.71	n.d.	n.d.	0.051	35.282	0.026	27.93	n.d.	0.02	0.001	n.d.	100.02	41.5
	Ol	40.79	n.d.	n.d.	0.097	9.984	0.566	47.75	0.025	0.002	0.012	n.d.	99.227	10.5
3	Rgt	33.18	n.d.	0.003	0.033	56.37	0.057	9.931	n.d.	0.006	0.003	n.d.	99.581	76.1
	Ol	41	0.015	n.d.	0.024	11.603	0.363	46.66	0.046	n.d.	n.d.	n.d.	99.711	12.2
4	Rgt	38.28	n.d.	0.044	0.007	33.108	0.048	29.44	0.011	0.015	n.d.	n.d.	100.95	38.7
	Ol	41.38	0.001	n.d.	n.d.	9.769	0.132	48.74	0.001	n.d.	n.d.	n.d.	100.02	10.1
5	Rgt	36.43	0.042	0.933	0.34	36.8	0.206	24.67	0.354	0.355	0.01	n.d.	100.14	45.6
	Ol	40.76	n.d.	0.004	n.d.	9.503	0.39	49.51	0.041	0.017	n.d.	0.021	100.25	9.7
6	Rgt	35.23	n.d.	n.d.	0.076	44.4	0.041	21.6	n.d.	0.03	n.d.	n.d.	101.37	53.6
	Ol	41.52	n.d.	n.d.	0.042	6.366	0.429	51.7	0.031	n.d.	n.d.	n.d.	100.09	6.5
7	Rgt	37.4	n.d.	0.117	0.024	27.27	0.119	35.47	n.d.	n.d.	n.d.	0.006	100.4	31.0
	Ol	40.19	0.018	n.d.	0.021	8.315	0.268	51.57	0.018	0.007	0.007	n.d.	100.41	8.3
8	Rgt	35.74	n.d.	0.11	0.087	36.28	0.029	28.08	n.d.	0.024	0.019	n.d.	100.37	42.0
	Ol	40.67	n.d.	n.d.	0.047	8.352	0.194	51.5	n.d.	0.004	0.007	n.d.	100.77	8.3

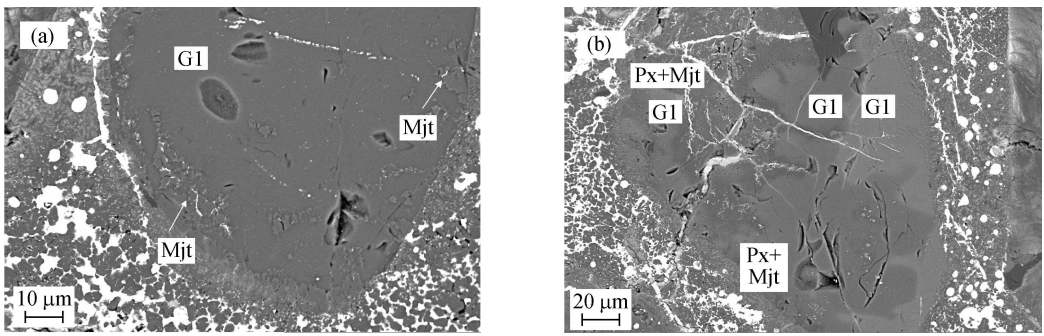

Fig. 9 (a) Back-scattered electron (BSE) image of a shock-induced vein in GRV 052049, showing a large pyroxene grain being transformed into majorite (Mjt) and glass (Gl). The scale bar is 10 μm.
(b) Back-scattered electron (BSE) image of a shock-induced vein in GRV 052049. The clast consists of pyroxene (Px), majorite (Mjt) and pyroxene glass (Gl). The scale bar is 20 μm.

3.6 High-pressure polymorphs of plagioclase

Large grains of plagioclase have been observed in high-equilibrated samples of type 5

or 6. The plagioclase are generally pure white transparent crystals with clear outlines. In heavily shocked samples, some plagioclase grains exhibit complete extinction under cross-polarized light, which indicates that the texture of these grains were destroyed during the shock pulse and transformed into isotropic glass.

Coarse-grained plagioclase were also found in host-rock fragment entrained in shock-induced veins. These grains, which display full extinction under cross-polarized light, are smooth and lack of cleavage, cracks, and fractures on BSE image. They commonly coexist with ringwoodite and majorite. Raman analyses on these grains reveal that most of them are maskelynite. However, Raman mode around 760 cm^{-1} was detected in a few grains, which revealed the existence of lingunite, a high-pressure modification of feldspar that possesses the tetragonal hollandite structure. Natural occurrence of lingunite was first reported in Sixiangkou meteorite, indicative of the P-T conditions of 21—24 GPa at 2000℃.

4 Discussion

4.1 High-pressure minerals and P-T history

High-pressure minerals and assemblages were observed in 17% of samples. The coarse-grained olivine aggregates in the shock-induced veins are partially transformed into ringwoodite with high Fa contents, while the coexisting olivine grains always exhibit lower Fa contents than that of the olivine in the host rock. The shocked samples are all highly equilibrated type 5 or 6, the host rock silicates exhibiting relatively homogeneous chemical compositions. The wide compositional gap between ringwoodite and coexisting olivine suggests that under the homogeneous pressures, the cation diffusion between olivine and ringwoodite are highly controlled by the temperature gradients in the grains (low temperature in interiors and high temperature in rims), and requires a long duration time of the high pressures and temperatures after the pulse of shock wave.

EMPA results show that the FeO-enriched crystallites (< 1 μm) embedded in the grey matrix have chemical compositions of olivine. On BSE image, they display the same brightness as ringwoodite, which is much higher than the olivine in the host rock. However, no typical ringwoodite peak was detected by Raman spectrometer, probably due to the tiny size of the ringwoodite crystallites, or the back-transformation of ringwoodite into olivine, while remaining the high FeO content.

Maskelynite could be found in both host rock and shock-induced veins, whereas the maskelynite in the shock-induced veins exhibits an allomorphic outline, that maskelynite usually fills fractures and cracks in other nearby silicate minerals. Chromite inclusions were commonly observed in maskelynite. Due to the polygonal outlines of the trapped chromite, and higher melting point of chromite than plagioclase (2000℃ *vs* 1100℃), it's very unlikely that the chromite inclusions were crystallized from melt which were formed during shock event from original chromite and dissolved into feldspar melt. Brickle chromite grains were easily to be broken into pieces by impact, which were captured by the melted plagioclase glass. These features suggest that the maskelynite in shock-induced vein is not diaplectic plagioclase glass formed by solid-state transformation, but a dense quenched glass

from plagioclase melt that formed at ~ 20 GPa, > 1100℃.

According to the results of shock-loading experiments in Allende meteorite, the ringwoodite + (Mg, Fe)SiO_3-Majorite assemblages observed in several samples were formed at 18—23 Gpa, 1800—1900℃. Besides, (Mg, Fe)SiO_3-glass were identified in a few heavily shocked samples. The occurrence of (Mg, Fe)SiO_3-glassy phase in this study is identical to that reported from Suizhou meteorite, which was considered as vitrified perovskite during the decompression stage due to a high post-shock temperature. Pyroxene could transform into perovskite at high pressures but a relatively low temperature (23—25 Gpa, 2000℃). However, the heating experiments and the molecular- and lattice-dynamics calculations indicated that the crystalline $MgSiO_3$ perovskite would be decompressed to an amorphous phase near the ambient pressure from its high-pressure stability fields at modest temperatures. The vitrification of $MgSiO_3$ perovskite begins above 127℃ and is complete by 477 ℃ at ambient pressure[13]. After the peak of shock pulse, the post-shock temperature in these samples must have been higher than 477 ℃, inducing a rapid vitrification of crystalline perovskite into (Mg, Fe)SiO_3-glass. Therefore, the existence of vitrified perovskite indicates that the peak pressure in the shock veins exceeds 23 GPa.

4.2 *Classification and distribution of Shock Stages*

A petrographic classification of progressive stages of shock metamorphism of ordinary chondrites were put forward by Stöffler *et al.* and widely used afterwards. According to his classification, seven stages of shock (S1-S6 and shock melted) were defined based on the shock effects in the main silicate components as recognized by thin section microscopy. A shock pressure calibration for the S1-S6 stages was also proposed (Table 2), in which the occurrence of high-pressure polymorphs as ringwoodite, majorite, maskelynite were taken as an indicator of shock stage S6, and a extremely high pressure of 75—90 GPa.

Table 2 Classification of Shock Stages of Ordinary Chondrites (Base on literature [2])

Shock Stage	Silicates			Local effects	Shock pressure (Gpa)
	Olivine	Pyroxene	Plagioclase		
S1	sharp optical extinction, irregular fractures			none	< 4—5
S2	undulose extinction, irregular fractures			none	5—10
S3	planar fractures undulose extinction, irregular fractures			opaque shock veins, incipient formation of melt pocekts	10—15
S4	planar fractures weak mosaicism partially isotropic			opaque shock veins and melt pockets interconnecting	25—30
S5	planar fractures strong mosaicism maskelynite			pervasive melt pockets and shock veins	45—60
S6	in or near the shock induced-veins, solid state recrystallization of silicates ringwoodite majorite normal glass			pervasive melt pockets and shock veins	75—90

With the development of high-pressure experiments and study in shock metamorphism in meteorites, modification and correction were made on the P-T-t conditions and formation history of high-pressure minerals in meteorites. Accordingly, modification and revise are needed for the current classification and pressure calibration system of shock stages in ordinary chondrites. In this study, we have classified the shock stages of 93 Grove Mountains ordinary chondrites (results listed in Table 3). The classification was mainly on the basis of Stöffler's scheme, while shock effects including optical properties of silicates, shock-induced localized melting and high-pressure transition of minerals were also taken into consideration.

Table 3. shock metamorphism grades of Grove Mountains ordinary chondrites (Base on literature [2])

Shock Stage	Silicates			Local effects	Results
	Olivine	Pyroxene	Plagioclase		
S1	sharp optical extinction, irregular fractures			none	6
S2	undulose extinction, irregular fractures			none	47
S3	planar fractures undulose extinction, irregular fractures (a few ringwoodite)			opaque shock veins; incipient formation of melt pocekts	17
S4	planar fractures weak mosaicism ringwoodite maskelynite			opaque shock veins and melt pockets interconnecting	18
S5	planar fractures strong mosaicism ringwoodite majorite maskelynite (a few $(Mg, Fe)SiO_3$-glass)			pervasive melt pockets and shock veins	5
S6	in or near the shock induced-veins, solid state recrystallization of silicates			pervasive melt pockets and shock veins	0

We now compare the various frequency distributions of shock stages within different chemical groups and petrologic types of the samples in this study (Fig. 10).

A conspicuous difference between L and H group can been seen. L chondrites appear to have a larger fraction of shocked samples, as there are more the L chondrites shocked to S3-S5 than the weakly or unshocked ones (34 *vs* 22), while the shock metamorphism is not so extensively developed in H group chondrites. Most of H chondrites were weakly shocked (29 of 43 samples), except for only one samples was classified as S4.

Stöffler *et al* have studied the shock metamorphism in 35 H group, 27 L group and 14 LL group chondrites. Their results showed that the differences in the frequency distribution of shock stages in H, L and LL groups are minor; besides, the shock effects and the sequence of progressively increasing degrees of shock metamorphism are very similar. However, the investigation of the Meteoritical Bulletin Database suggests that the frequency distributions of shock stages between L and H groups are different. There are 23 L group chondrites of all the chondrites that were shocked to S4—S6, whereas the number of H group is 9. It's evident that the L group chondrites have experienced stronger shock metamorphism than H group, which is in consistent with our results in this study.

The frequency of shock stages within different petrologic types (Fig. 10b) reveals some similar variations. With increasing petrologic type, the frequency of shock stages S3, S4, and S5 increases. Shock stage S2 is the most abundant in nearly all petrologic types. It appears that type 3 ordinary chondrites are deficient in shock stages S3 to S5. There is a lack of shock stages S4 and S5 in petrologic type 3 and 4 chondrites in contrast to type 5 and 6 chondrites.

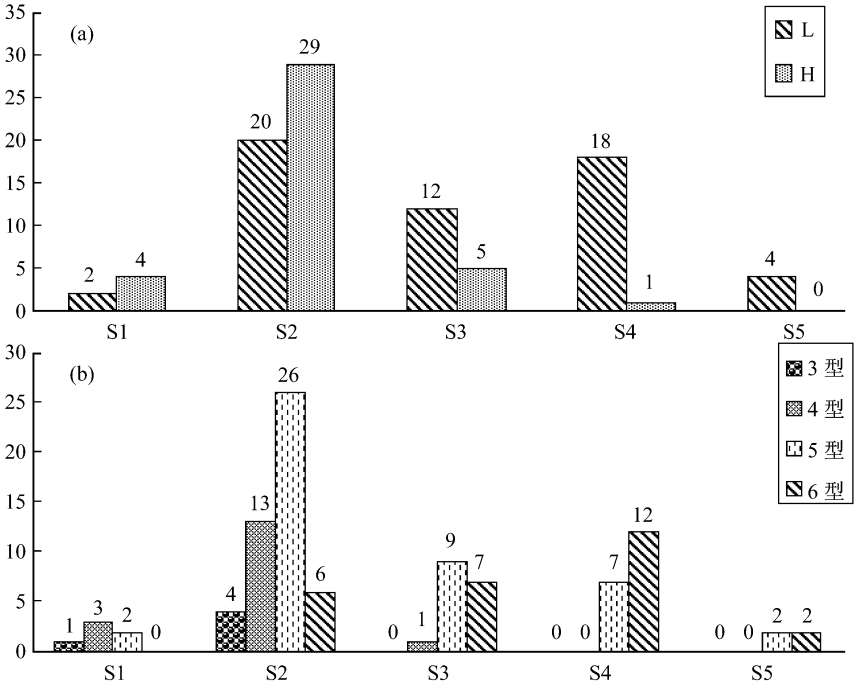

Fig. 10. Histograms of shock grades of Grove Mountains ordinary chondrites, based on (a) chemical groups, and (b) petrographic types.

The tendency between petrologic types and shock stages, that heavily shocked samples are most likely to be observed in highly equilibrated ordinary chondrites, may be attributed to the different physical properties of all the types of chondrites in the unshocked state. High equilibrated samples (type 5/6 chondrites) are essentially coherent nonporous rocks, in which the high pressures and temperatures are easier to be retained for a longer time during shock event, while the unequilibrated chondrites (type 3/4) are more porous and richer in volatiles which are more possible to be crushed by the impact, therefore the high pressure would be released. In another aspect, since different groups of chondrites come from different parent bodies, the diverse distribution of frequencies of shock stages between H and L groups may result from the different physical properties of the surfaces of their parent bodies, for example, the thickness of soil layer, the petrologic type of rocks on the surface *etc.* As we discussed above, thick and porous soil layer is not favorable to reserve high pressure and temperature conditions. An analogous case can be seen on the moon and Mars. The former is covered by a layer of lunar regolith of 2—10 m in depth, while Martian soil is not so abundant on the surface of Mars, especially in the Tharsis bulge region. Cor-

respondingly, high-pressure transitions were not commonly reported to be discovered in lunar meteorites which exhibit shock effects, while high-pressure polymorphs as maskelynite and stishovite were found in several shergotty Martian meteorites.

5 Conclusion

Shock effects of 93 Grove Mountains ordinary chondrites were studied and described. High-pressure minerals as Ringwoodite, maskelynite, majorite, majorite-pyrope solid solution and $(Mg, Fe)SiO_3$ glass, which is supposed to be vitrified $(Mg, Fe)SiO_3$ perovskite, were identified in shock-induced veins. Based on the coexistence of high-pressure polymorphs, the peak pressure of the shock event was up to 23 GPa, while the temperatures may have exceeded 2000℃. The olivine clasts enclosed in the shock-induced vein were partly transformed into ringwoodite. There is obvious enrichment or depletion in Fe and Mg contents between ringwoodite and coexisting olivine, respectively, which may represent the diffusion of elements during the shock event, and a long duration of the high pressure pulse.

On the basis of the observed shock effects, shock stages of the 93 Grove Mountains ordinary chondrites were classified. There are 6 of shock stage S1, 47 of S2, 17 of S3, 19 of S4 and 4 of S5. Comparison the frequencies of shock stages within different chemical groups shows a diverse frequency distribution of shock stages between H and L groups, which may represent the difference between physical properties of the surfaces of their parent bodies. Besides, it appears with increasing petrologic type, the frequency of shock stages S3, S4, and S5 increases.

Acknowledgements We thank the Polar Research Institute of China to have provided all the samples in this study. This study was supported by the Knowledge Innovation Program of the Chinese Academy of Sciences (kzcx2-yw-110, KZCX2-YW-Q08).

References

[1] Dodd R T, Jarosewich E (1979): Incipient melting in and shock classification of L-group chondrites. Earth Planet Science Letter, 44: 335–340.

[2] Stöffler D, Keil K, Scott E R D (1991): Shock metamorphism of ordinary chondrites. Geochimica et Cosmochimica Acta, 55: 3845–3867.

[3] Chen M, Sharp T G, El Goresy A *et al* (1996): The majorite-pyrope + magnesiowüstite assemblage: constraints on the history of shock veins in chondrites. Science, 271: 1570–1573.

[4] Gillet P, Chen M, Dubrovinsky L *et al* (2000): Natural $NaAlSi_3O_8$-hollandite in the shocked Sixiangkou meteorite. Science, 287: 1633–1636.

[5] Xie Z, Sharp T G, De Carli P S (2006): High-pressure phases in shock-induced melt veins of the Tenham L6 chondrite: Constraints of shock pressure and duration. Geochemica et Cosmochimica Acta, 70: 504–515.

[6] Rubin A E, Scott E R D, Keil K (1997): Shock metamorphism of enstatite chondrites. Geochimica et Cosmochimica Acta, 61(12): 847–858.

[7] Xie X, Chen M, Wang D (2001): Shock-related mineralogical features and P-T history of the Suizhou L5 chondrite. European Journal of Mineralogy, 13: 1177–1190.

[8] Katsura T, Yamada H, Nishikawa O *et al* (2004): Olivine-wadsleyite transition in the system (Mg

Fe)$_2$SiO$_4$. Journal of Geophysics Research, 109: B02209.
[9] Inoue T, Irifune T, Higo Y *et al.* (2006): The phase boundary between wadsleyite and ringwoodite in Mg$_2$SiO$_4$ determined by in situ X-ray diffraction. Phys Chem Minerals, 33: 106–114.
[10] Mcmillan P, Akaogi M (1987): Raman spectra of β-Mg$_2$SiO$_4$ (modified spinel) and γ-Mg$_2$SiO$_4$ (spinel). American Mineralogist, 72: 361–364.
[11] Malavergne VGF, Benzerara K, Martinez I (2001): Description of new shock-induced phases in the Shergotty, Zagami, Nakhla, and Chassigny meteorites. Meteoritics & Planetary Science, 36: 1297–1350.
[12] Tomioka N, Kimura M (2003): The breakdown of diopside to Ca-rich majorite and glass in a shocked H chondrite. Earth and Planetary Science Letters, 208: 271–278.
[13] Chen M, Xie X, El Goresy A (2004): A shock-produced (Mg, Fe)SiO$_3$ glass in the Suizhou meteorite. Meteoritics & Planetary Science, 39: 1797–1808.
[14] Trukhin A CB (2005): Raman and optical reflection spectra of germanate and silicate glasses. Journal of Non-Crystalline Solids, 351: 3640–3643.
[15] Yagi A, Suzuki T, Akaogi M (1994): High pressure transitions in the system KAlSi$_3$O$_8$-NaAlSi$_3$O$_8$. Physics and Chemistry of Minerals, 21: 12–17.
[16] Tutti F (2007): Formation of end-member NaAlSi$_3$O$_8$ hollandite-type structure (lingunite) in diamond anvil cell. Physics of The Earth and Planetary Interiors, 161(3—4): 143–149.
[17] Xie XD, Chen M, Wang DQ *et al.* (2006): Melting and vitrification of plagioclase under dynamic high pressures. Acta Petrologica Sinica, 022: 503–509.
[18] Chen M, El Goresy A (2000): The nature of maskelynite in shocked meteorites: not a diaplectic glass but a glass from shock-induced dense melt at high pressure. Earth and Planetary Science Letters, 179: 485–502.
[19] Agee CB, Li J, Shannon MC *et al.* (1995): Presure-temperature phase diagram for the Allende meteorite. Journal of Geophysics Research, 100: 17725–17740.